



Eye Diseases Classification Using Back Propagation Artificial Neural Network

Hanaa M. Ahmed ^a, Shrooq R. Hameed ^{b*}

^a Department of Computer Science, University of Technology, Baghdad, Iraq,
110113@uotechnology.edu.iq.

^b Department of Computer Science, University of Technology, Baghdad, Iraq,
shrooq_rasheed@yahoo.com.

*Corresponding author.

Submitted: 26/11/2019

Accepted: 24/04/2020

Published: 25/03/2021

KEY WORDS

Back Propagation, Eye Diagnosis, Feature Extraction, Hue, Min, Max, Diff (HMMD) color space, Laws Feature.

ABSTRACT

A human eye is a vital organ responsible for a person's vision. So, the early detection of eye diseases is essential. The objective of this paper deals with diagnosing of seven different external eye diseases that can be recognized by a human eye. These diseases cause problems either in eye pupil, in sclera of eye or in both or in eyelid. Color histogram and texture features extraction techniques with classification technique are used to achieve the goal of diagnosing external eye diseases. Hue Min Max Diff (HMMD) color space is used to extract color histogram and texture features which were fed to Back Propagation Artificial Neural Network (BPANN) for classification. The comparative study states that the features extracted from HMMD color space is better than other features like Histogram of Oriented Gradient (HOG) features and give the same accuracy as features extracted directly from medical expert recorded symptoms. The proposed method is applied on external eye diseases data set consisting of 416 images with an accuracy rate of 85.26315%, which is the major result that was achieved in this study.

How to cite this article: H. M. Ahmed, and S. R., Hameed, "Eye Diseases Classification Using Back Propagation Artificial Neural Network," Engineering and Technology Journal, Vol. 39, Part B, No. 01, pp. 11-20, 2021.

DOI: <https://doi.org/10.30684/etj.v39i1B.1363>

This is an open access article under the CC BY 4.0 license <http://creativecommons.org/licenses/by/4.0>

1. INTRODUCTION

The human eye is the most important organ among the five senses, so early detection of external eye diseases has become an important issue in medicine. Pattern recognition has a wide area of applications. One of these applications is in the medical field. Early detection of eye diseases prevents the diseases to become more complicated. It also reduces the burden in the

hospitals, as well as it enables people far away from hospitals to check the health of their eyes and take the necessary actions to prevent the worsening of eye disease conditions.

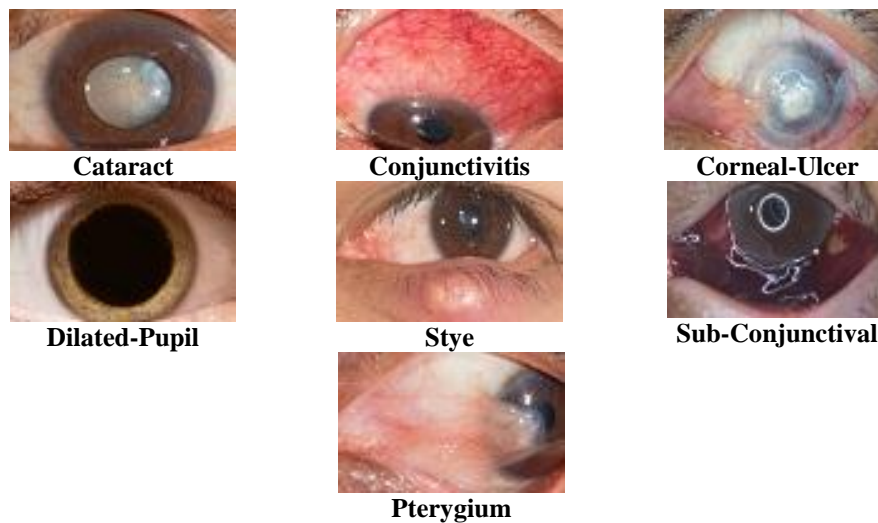


Figure 1: Seven External Eye Diseases.

Machine learning has proved that it has the ability to produce very good accuracy in diagnosing different medical conditions like chests X-ray, breast cancer, and many others. [1]

This paper classifies seven different external eye diseases (Cataract, Conjunctivitis, Corneal-Ulcer, Dilated-Pupil, Stye, Sub-Conjunctival, and Pterygium) as seen in Figure 1. First, eye image is converted from (Red, Green, and Blue) RGB color space into HMMMD color space. Second, non-linear quantization is applied on the resultant image. Third, histogram features besides texture features using Law features are extracted. Lastly, these features are fed into Back Propagation for classification purposes.

This paper is organized as follows: In section 2, related work is discussed. In section 3, two types of feature extraction methods are discussed, while Architecture of Back Propagation used in this paper explained in details in section 4. The methodology used in this paper explained in section 5. Results & discussions presented in section 6. Finally, conclusions are illustrated in section 7.

2. RELATED WORK

Many studies were completed for diagnosing eye diseases, different feature extraction techniques and classification algorithms were developed in these studies. Some of them are discussed in this section, such as Cost-Sensitive deep residual convolutional neural network classifier was used to diagnose ophthalmic diseases using retro-illumination images in [2]. Only two kinds of eye diseases (Cataract, Conjunctivitis) were recognized through HOG features which classified by using minimum distance classifier in [3]. In another article, five eye diseases were selected to be classified utilizing HOG features with Artificial Neural Network [4]. Whereas, in Ref [5] medical expert recorded symptoms directly in the form of standard taxonomies from which features were extracted and four different classification methods (Decision Tree, Naive Bayesian, Random Forest, and Neural Network) applied on these features to identify eye diseases. Instead, Hybrid approach was implemented in [6], known as Neural Networks Decision Trees, where symptoms and physical eye conditions learned with neural network to acquire rules were fed to Decision Tree in order to diagnosis the eye diseases. Finally, Gray Level Co-occurrence Matrix (GLCM) was used to extract features that fed to Bayesian Regularization Back-Propagation Neural Network (BRBPNN) classifier to identify Corneal Arcus in [7].

3. FEATURE EXTRACTION

Feature extraction is the process of reducing the dimensions of an image to describe the image according to the extracted features. Different features can be extracted from the same image according to different feature extraction methods [8].

1. HMMD Color Space

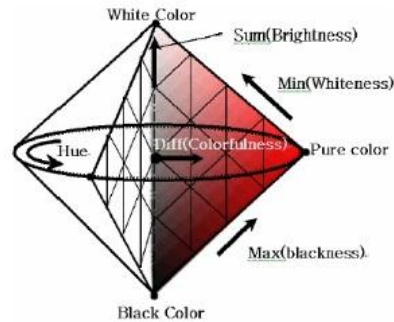


Figure 2: HMMD Color Space.[9]

HMMD is a more perceptual uniform color space. It stands for Hue (same as Hue in HSV (Hue Saturation Value) color space) Min, Max, Diff are the result of transform equations from RGB into HMMD color space.

$$Min = \min(R, G, B) \quad (1)$$

$$Max = \max(R, G, B) \quad (2)$$

$$Diff = Max - Min \quad (3)$$

In addition to these three equations, another component was defined is sum and its equation as follows:

$$sum = (Max + Min)/2 \quad (4)$$

HMMD color space has the shape of double cone as shown in Figure 2, and it can be defined from three of five components, either by Hue, Diff, and Sum (HDS) or by Hue, Max, and Min (HMM). As mentioned previously Hue is the same as in HSV color space, while Diff has the same property of Saturation in HSV color space, and Sum gives the brightness of the color [9].

1) HMMD Color Space Quantization

Four color space quantization points were defined on the HMMD color space: 256, 128, 64, and 32 bins. The quantization process as shown in Table I does as follows: HMMD color space is divided into five sub-spaces according to Diff component by the following intervals: [0, 6], [6, 20], [20, 60], [60,110], and [110, 255]. Then, each of these color sub-spaces are quantized uniformly depending on Hue and Sum components, where the quantization level of these component is determined[10].

TABLE I: HMMD Color Space Quantization.[10]

| Component | Sub-Space | Number of Quantization Levels for Different Numbers of Histogram Bins | | | |
|-----------|-----------|---|-----|----|----|
| | | 256 | 128 | 64 | 32 |
| Hue | 0 | 1 | 1 | 1 | 1 |
| | 1 | 4 | 4 | 4 | 4 |
| | 2 | 16 | 8 | | |
| | 3 | 16 | 8 | 8 | 4 |
| | 4 | | | | |

| | | | | | |
|-----|---|----|----|---|---|
| Sum | 0 | 32 | 16 | 8 | 8 |
| | 1 | 8 | 4 | 4 | 4 |
| | 2 | 4 | | | |
| | 3 | 4 | 4 | 2 | 1 |
| | 4 | | | 1 | |

II. Laws Features

There are many approaches for extracting texture features. One of them is Law Mask texture features; it was created by Kenneth Ivan Laws in 1980. Laws features extracted by applying convolution operation between certain mask and the image to extract specific texture properties from the image. These masks obtained by combining one dimensional kernel .[11, 12] Laws combines five labeled vectors to form 2D kernel mask, each mask responsible of extracting certain property from the image when it convolved with that image.[13] The vectors are L5=[1 4 6 4 1] to enhance Intensity Level, E5=[-1 -2 0 2 1] to enhance Edges, S5=[-1 0 2 0 1] to enhance Spots, R5=[1 -4 6 -4 1].to enhance Ripples, and W5=[-1 2 0 -2 1] to enhance Waves.[14] The cross product of these five vectors in the horizontal and vertical directions to produce 25 2-D convolutional masks.[14]

4. BPANN

BPANN is one of Artificial Neural Network most popular methods used to optimize Feed Forward Neural Network training due to its flexibility, competence, and solve problems in many situations such as pattern recognition, function approximation, pattern matching, and associative memories,[15] since it is robust, fault-tolerance, and parallel solution. It is allow learning information collected from different sources or kinds.[16] BPANN is a supervised Learning Algorithm, in which the input is processed to map the desired output by reducing the error between the desired output and the calculated output driven from the inputs and the network learning.[17] with feed forward architectures, three different layers are constructed. Input layer, is a set of input neurons which accept input elements fully connected to the hidden neurons in the hidden layer. Hidden Layer, in turn, is fully connected to the output neurons in the output layer. The response of the neural network produced by the output layer is back propagated to the activation neurons in the hidden layer. In general, the information that feed to the neural network is propagated forward and backward layer by layer between input layer and output layer. [18] Weights are associated with each connection between input and hidden layers and between hidden and output layers. These weights determine the strength of the input vector. If the weight is positive, it excite the node output. If the weight is negative, it inhibit the node output.[18] The aim of the back propagation function is to reduce the error function in weight space by the gradient descent. This requires, at each step, the gradient of the error function must be computed in order to guarantee the continuity and differentiability of the error function. The structure of BPANN of two layers explained in Figure 3.

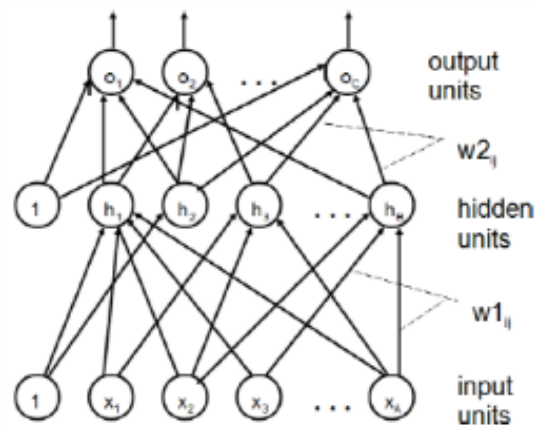


Figure 3: The Structure of 2-layer BPANN.[16]

Some of activation functions that provide the above conditions are sigmoid function, symmetrical sigmoid function, hyperbolic function, and others.[19] Symmetrical sigmoid function used in this paper is defined by the following equation:

$$y = \frac{1 - e^{-net}}{1 + e^{-net}} \quad (5)$$

And its shape is shown in the Figure 4 below.

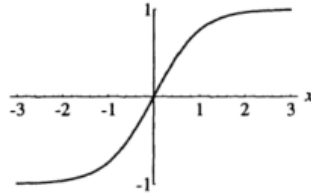


Figure 4: The Graph of the Symmetrical Sigmoid Function.[19]

$$net_j^h = \left(\sum_{i=1}^A W_{ij}^1 X_i \right) + b_j \quad (6)$$

where, w_{ij}^1 is the weight of the connection between neuron i in the input layer and neuron j in the hidden layer. net_j^h is the result of activation function for the j^{th} hidden neuron. b_j is the bias for the j^{th} neuron.

$$net_j^o = \left(\sum_{i=1}^B W_{ij}^2 y_i \right) + b_j \quad (7)$$

where, w_{ij}^2 is the weight of the connection between neuron i in the hidden layer and neuron j in the output layer. net_j^o is the result of activation function for the j^{th} output neuron.

To assess the accuracy of the neural network, the mean square error quantifies the amount by which the estimated output differs from the desired output which, known as the error. Mean square error is widely used as a cost function in neural network due to its good performance in large datasets on real world problems.[20] The objective of back propagation is to minimize the neural network error described by the following equation.

$$E = \frac{1}{2} \sum_{i=1}^n (y_i - d_i)^2 \quad (8)$$

where, n is the number of network output. y_i is the i^{th} output of the network. d_i is the i^{th} desired output of the network.

The learning process of back propagation algorithm is an optimization problem that aims at finding the weight coefficients for a given training set. First of all, the weights are chosen randomly in range between (0, 1). Secondly, the training data are fed to the input neuron. Then, the output of the hidden layer and output layer are calculated according to the equations (6) and (7) respectively. The error between the network output and the desired output is calculated according to the equation (8), while the error for the output layer calculated according to the equation (9) [21].

$$\delta_i^o = y_i^o (y_i^o - d_i) (1 - y_i^o) \quad (9)$$

where, δ_i^o is the error of the i^{th} output neuron. y_i^o is the i^{th} output neuron, and the error for the hidden layer is calculated according to the equation (10).[21]

$$\delta_i^h = y_i^h(1 - y_i^h) \sum_{j=1}^C W_{ji}^2 \delta_j^o \quad (10).$$

where, δ_i^h is the error of the i^{th} hidden neuron. y_i^h is the output of the i^{th} hidden neuron. The weights modifications are calculated as follows:

$$\Delta w_{ij}(t) = \alpha \delta_i^l(t) y_j^{l-1} + \beta \Delta w_{ij}(t - 1) \quad (11).$$

where, Superscript l denotes the input layer while superscript $l - 1$ denotes the hidden layer in case of the input-hidden weight. While superscript l denotes the hidden layer and superscript $l - 1$ denotes the output layer in case of the hidden-output weight. α is the momentum term and β is the learning rate term. Lastly, t is the current iteration and $t - 1$ is the previous iteration.

The Bias modification for each neuron in hidden and output layers calculated as:[21]

$$\Delta B_i(t) = \alpha \delta_i(t) + \beta \Delta B_i(t - 1) \quad (12).$$

The new weights and new bias for each neuron in hidden and output layers are calculated as:[21]

$$w_{ij}(t + 1) = w_{ij}(t) + \Delta w_{ij}(t) \quad (13).$$

$$B_i(t + 1) = B_i(t) + \Delta B_i(t) \quad (14).$$

where, $t + 1$ is the next iteration.

5. THE PROPOSED METHOD

Seven external eye diseases (Cataract, Conjunctivis, Corneal-Ulcer, Dilated-Pupil, Stye, Sub- Conjunctival, and Pterygium) are classified in this paper. Figure 5 illustrates the block diagram of the proposed method. Data set of external eye diseases was taken from <https://www.shutterstock.com/>, in which each image is converted from RGB color space to HDS color space, as shown in Figure 1. Each disease can be recognized by both its color and its texture. For color features, the converted images quantized into 32-bins as mentioned in section I, then, the color histogram was computed. For texture features, laws texture features were utilized. 25-Masks of Laws texture features are applied to Sum channel of HDS. As a result, the feature vector consists of 49 feature points that were obtained. Before feeding the feature vectors into back propagation neural network, the mean and standard deviation of all feature vectors were computed and each feature point subtracted from the computed mean and divided by computed standard deviation in order to standardize the feature points as a pre-processing step. The data set is partitioned into training set and test set according to the ratio (80:20) respectively. Finally, neural network built with single hidden layer in addition to input and output layers using OPENCV-MLP (Multi-Layer Perceptron) in JAVA Programming Language. In which, the input layer consists of neurons equal to the number of features in feature vector, the output layer consists of neurons equal to the number of eye external diseases, while the number of neurons in the hidden layer are computed according to the following equation (15):

$$\text{no. of hidden neuron} = \frac{(\text{no. of input neuron} + \text{no. of hidden neuron})}{2} \quad (15)$$

The learning rate used is equal to (0.002), while the momentum term used is equal to (0.078). The error excepted is equal to (0.000001), and the number of iterations is equal to (1000).

6. RESULTS & DISCUSSIONS

The proposed method applies on seven external eye diseases that can be observed by a human eye only. These diseases cause problems either on eye pupil, sclera of eye, or both of them or on eye lid. Two types of features are used in this paper; color features and texture features. Table II shows HDS Color Histogram feature extraction is applied on a sample from

each disease. Table III shows Laws texture features extracted from a sample of each eye disease. Both of these features are normalized to have a unified scale (between 0 and 1) before feeding them to the network.

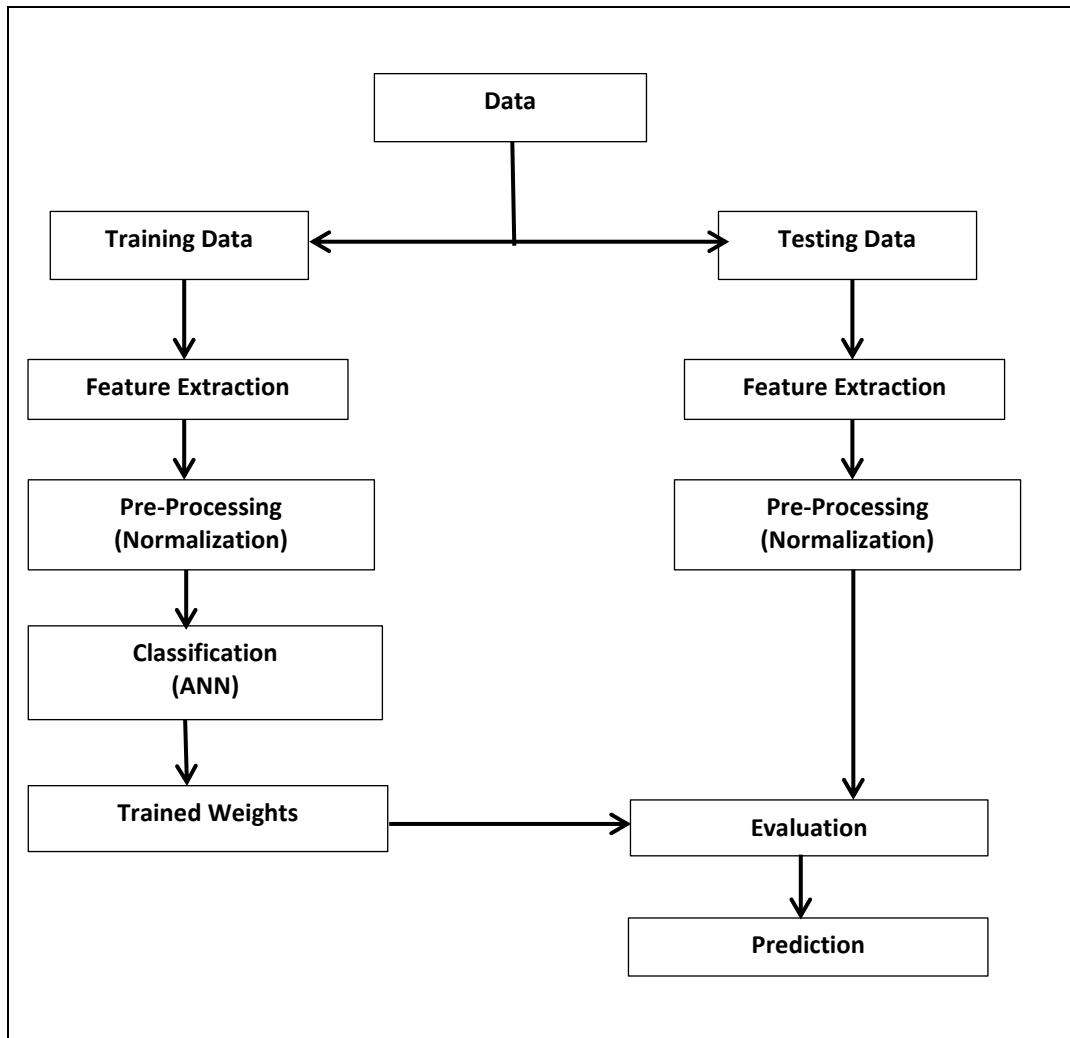


Figure 5: The Block Diagram of the Proposed Method.

The success of the neural network depends on making the predicted output the same as the desired output as much as possible using gradient descent. Experimental tuning the learning rate parameter did not lead to improvement in performance significantly. Precision of Stye and Dilated-Pupil diseases is 100%. Another two eye diseases (Corneal-Ulcer and Conjunctivitis) have a precision greater than 90%, while the other three eye diseases have precision lower than 90%. Cataract precision is about 60%, while Pterygium precision is about 85%, and Sub-Conjunctival precision is about 75%. The last three eye diseases precisions affect the overall classification performance. Increasing the size of data set can lead to improving the classification performance. The accuracy achieved by the proposed method is equal to 85.26315%, and F1-Score measurement is also utilized and gives 85.95%, while sensitivity equal to 85.5%, and, specificity equal to 87.44%. Comparative study between the proposed method and related work is presented in Table IV.

7. CONCLUSION

The proposed method illustrates that the features extracted from HMMD color space are better features that give higher accuracy than HOG features in (1) in Table IV. Also, features extracted from HMMD color space gives approximately the same classification accuracy as compared to (5) in Table IV. In the future, additional external eye diseases like Cyst, Glaucoma, Keratitis, and Uveitis can be added to be classification.

TABLE II: Color Histogram Feature Extraction of Seven Eye Diseases.

| Cataract | Conjunctivis | Corneal-Ulcer | Pterygium | Stye | Sub-Conjunctival | Dilated-pupil |
|----------|--------------|---------------|-----------|------|------------------|---------------|
| 62 | 0 | 0 | 60 | 82 | 0 | 125 |
| 29 | 0 | 15 | 25 | 4 | 25 | 24 |
| 14 | 0 | 1 | 11 | 0 | 31 | 14 |
| 58 | 1 | 0 | 3 | 0 | 3 | 9 |
| 36 | 0 | 0 | 3 | 0 | 0 | 6 |
| 15 | 2 | 0 | 0 | 0 | 0 | 34 |
| 39 | 0 | 0 | 1 | 0 | 0 | 1 |
| 396 | 0 | 1 | 930 | 169 | 1 | 765 |
| 158 | 276 | 63 | 250 | 322 | 86 | 95 |
| 206 | 48 | 46 | 75 | 264 | 129 | 0 |
| 202 | 4 | 0 | 4 | 32 | 0 | 0 |
| 0 | 0 | 0 | 44 | 5 | 3 | 512 |
| 9 | 0 | 0 | 2 | 0 | 90 | 230 |
| 193 | 0 | 0 | 3 | 0 | 16 | 100 |
| 4 | 0 | 0 | 2 | 0 | 0 | 14 |
| 76 | 0 | 93 | 216 | 8 | 57 | 226 |
| 390 | 34 | 874 | 25 | 6 | 627 | 48 |
| 858 | 13 | 5 | 5 | 0 | 70 | 150 |
| 96 | 9 | 0 | 7 | 2 | 14 | 114 |
| 80 | 0 | 56 | 208 | 5 | 80 | 67 |
| 283 | 544 | 376 | 28 | 1 | 112 | 3 |
| 119 | 468 | 98 | 56 | 1 | 195 | 1 |
| 25 | 131 | 1 | 0 | 1 | 1 | 0 |
| 0 | 21 | 335 | 687 | 2420 | 357 | 0 |
| 0 | 0 | 0 | 0 | 0 | 0 | 6 |
| 5 | 0 | 0 | 0 | 0 | 4 | 50 |
| 0 | 1753 | 1177 | 4 | 1 | 892 | 0 |
| 0 | 0 | 9 | 619 | 29 | 199 | 0 |
| 0 | 0 | 0 | 0 | 0 | 0 | 0 |
| 0 | 0 | 0 | 0 | 0 | 0 | 29 |
| 0 | 49 | 203 | 0 | 0 | 361 | 0 |
| 62 | 0 | 0 | 60 | 82 | 0 | 125 |

TABLE III: Laws Textures Feature Extraction of Seven Eye Diseases.

| Cataract | Conjunctivis | Corneal-Ulcer | Pterygium | Stye | Sub-Conjunctival | Dilated-pupil |
|-----------|--------------|---------------|-----------|----------|------------------|---------------|
| 1752.7917 | 1565.85070 | 1100.7220 | 1452.144 | 1495.967 | 1546.809937 | 1070.3775 |
| 48 | 8 | 46 | 897 | 041 | | 63 |
| 2.82E+08 | 3.34976224E8 | 1.19E+08 | 2.50E+08 | 3.32E+08 | 2.26E+08 | 1.31E+08 |
| 37.872154 | 43.7327842 | 35.548973 | 37.09519 | 35.77283 | 54.54650116 | 51.434291 |
| 24 | 7 | 08 | 958 | 859 | | 84 |
| 169136.54 | 189746.062 | 121805.98 | 140036.7 | 162473.5 | 295794.7188 | 359959.03 |
| 69 | 5 | 44 | 5 | 156 | | 13 |
| 50.951988 | 49.9149513 | 33.850204 | 42.42304 | 47.81344 | 47.82057571 | 37.277915 |
| 22 | 2 | 47 | 611 | 223 | | 95 |
| 220619.18 | 249443.218 | 94894.062 | 183024.2 | 249168.7 | 184751.7031 | 169890.90 |
| 75 | 8 | 5 | 813 | 813 | | 63 |
| 66.801643 | 121.563240 | 101.68943 | 71.74375 | 138.3105 | 117.659256 | 86.842796 |
| 37 | 1 | 79 | 916 | 621 | | 33 |

| | | | | | | |
|------------------|-------------|-------------|-------------|-------------|-------------|-------------|
| 623046.1875 | 1718910.875 | 963024.75 | 584662.5625 | 1813844.625 | 1608470.25 | 1057172.875 |
| 356.6337585 | 316.7009583 | 238.7914886 | 291.4016418 | 298.3064575 | 339.276001 | 249.5064545 |
| 1.01E+07 | 9736398 | 4532998.5 | 8286297 | 9802411 | 8926314 | 6852615 |
| 233.862548828125 | 238.6282654 | 152.8076782 | 192.8765411 | 222.8677673 | 235.5508881 | 159.1893005 |
| 5160179 | 6595645 | 2033148 | 3893909.75 | 6426292 | 4630331 | 2839480.75 |
| 216.3278503 | 323.6425171 | 178.3393707 | 169.7722931 | 325.1549988 | 277.8200378 | 214.234024 |
| 5170109 | 1.11E+07 | 2682262.75 | 2455534 | 1.06E+07 | 6640234 | 7509961.5 |
| 36.35089111 | 59.6106987 | 46.43264771 | 38.13827133 | 55.77558136 | 59.61948013 | 53.03539276 |
| 133086.0625 | 397138.5625 | 191232.7344 | 142320.2031 | 270872.7813 | 363257.125 | 456602.0938 |
| 25.67764091 | 43.33607864 | 35.50068665 | 26.96323776 | 42.49135971 | 42.19835281 | 39.90260696 |
| 71035.92188 | 199673.3281 | 115586.7109 | 73586.28125 | 159945.8594 | 191009.7813 | 312909.6563 |

TABLE IV: Comparative Study.

| Index | Author | Used Method | Obtained Accuracy |
|-------|--------|--|-------------------|
| 1. | [4] | Artificial Neural Network learned on HOG features | 77% |
| 2. | [5] | Decision Tree learned on patient symptoms | 85.81% |
| 3. | [5] | Naïve Bayes learned on patient symptoms | 81.53% |
| 4. | [5] | Random Forest learned on patient symptoms | 86.63% |
| 5. | [5] | Neural Network learned on patient symptoms | 85.98% |
| 6. | [6] | Neural Networks trained on (patient complain, symptoms and eye condition or cause) to extract rule for Decision Trees | 92% |
| 7. | [7] | BRBPNN applied on GLCM features | 96% |
| 8. | Our | BPANN learned on (HDS+Laws) features | 85.26315% |

References

- [1] D. S. W. Ting, L. R. Pasquale, L. Peng, J. P. Campbell, A. Y. Lee, R. Raman, *et al.*, "Artificial intelligence and deep learning in ophthalmology," *British Journal of Ophthalmology*, vol. 103, pp. 167-175, 2019.

- [2] J. Jiang, X. Liu, K. Zhang, E. Long, L. Wang, W. Li, *et al.*, "Automatic diagnosis of imbalanced ophthalmic images using a cost-sensitive deep convolutional neural network," *Biomedical engineering online*, vol. 16, p. 132, 2017.
- [3] M. Manchalwar and K. Warhade, "Detection of Cataract and Conjunctivitis Disease Using Histogram of Oriented Gradient," *International Journal of Engineering and Technology (IJET)*, 2017.
- [4] S. Desai, Z. Maurer, and C. Sidrane, "Drashtikon: Extra Ocular Disease Classification," 2016.
- [5] S. Malik, N. Kanwal, M. N. Asghar, M. A. A. Sadiq, I. Karamat, and M. Fleury, "Data Driven Approach for Eye Disease Classification with Machine Learning," *Applied Sciences*, vol. 9, p. 2789, 2019.
- [6] L. Kabari and E. Nwachukwu, "Neural networks and decision trees for eye diseases diagnosis," *Advances in Expert Systems*, pp. 63-84, 2012.
- [7] R. A. Ramlee, M. Hanafi, S. Mashohor, and Z. M. Noh, "Comparison of Classifiers for Detecting the Corneal Arcus as a Symptom of Hyperlipidemia," *Eye*, vol. 135, p. 135, 2016.
- [8] M. Claro, L. Santos, W. Silva, F. Araújo, N. Moura, and A. Macedo, "Automatic glaucoma detection based on optic disc segmentation and texture feature extraction," *CLEI Electronic Journal*, vol. 19, pp. 5-5, 2016.
- [9] J. Ohm, L. Cieplinski, H. Kim, S. Krishnamachari, B. Manjunath, and D. Messing, "Color descriptors: Introduction to MPEG-7–Multimedia content description interface (pp. 187–212)," ed: New York: Wiley, 2002.
- [10] A. Buturovic, "MPEG 7 Color Structure Descriptor for visual information retrieval project VizIR 1," 2005.
- [11] S. Dash and U. R. Jena, "Texture classification using steerable pyramid based Laws' masks," *Journal of Electrical Systems and Information Technology*, vol. 4, pp. 185-197, 2017.
- [12] R. Shenbagavalli and K. Ramar, "Classification of soil textures based on laws features extracted from preprocessing images on sequential and random windows," *Bonfring International Journal of Advances in Image Processing*, vol. 1, pp. 15-18, 2011.
- [13] H. A. Elnemr, "Statistical analysis of law's mask texture features for cancer and water lung detection," *International Journal of Computer Science Issues (IJCSI)*, vol. 10, p. 196, 2013.
- [14] [14] W. D. Gillett, "Image Classification Using Laws' Texture Energy Measures," 1987.
- [15] N. M. Nawi, A. Khan, and M. Z. Rehman, "A new back-propagation neural network optimized with cuckoo search algorithm," in *International conference on computational science and its applications*, 2013, pp. 413-426.
- [16] K. Suzuki, *Artificial neural networks: Architectures and applications: BoD–Books on Demand*, 2013.
- [17] Y. Huang, "Advances in artificial neural networks–methodological development and application," *Algorithms*, vol. 2, pp. 973-1007, 2009.
- [18] S. Mandal and I. Banerjee, "Cancer classification using neural network," *International Journal*, vol. 172, 2015.
- [19] R. Rojas, *Neural networks: a systematic introduction: Springer Science & Business Media*, 2013.
- [20] H. Rady, "Reyni's entropy and mean square error for improving the convergence of multilayer backpropagation neural networks: a comparative study," *International Journal of Electrical & Computer Sciences IJECS-IJENS*, vol. 11, pp. 68-79, 2011.
- [21] J. Stastny and V. Skorpil, "Neural networks learning methods comparison," *WSEAS Transactions on Circuits and Systems*, vol. 4, pp. 325-330, 2005.